

超高エネルギー宇宙線と

高エネルギー宇宙線一トリノ

理解への基礎的課題

高橋文郎

(理大院理)

2001. 7. 14

ICRR

◦ 超高エネルギー宇宙線

◦ AGN

◦ GRB

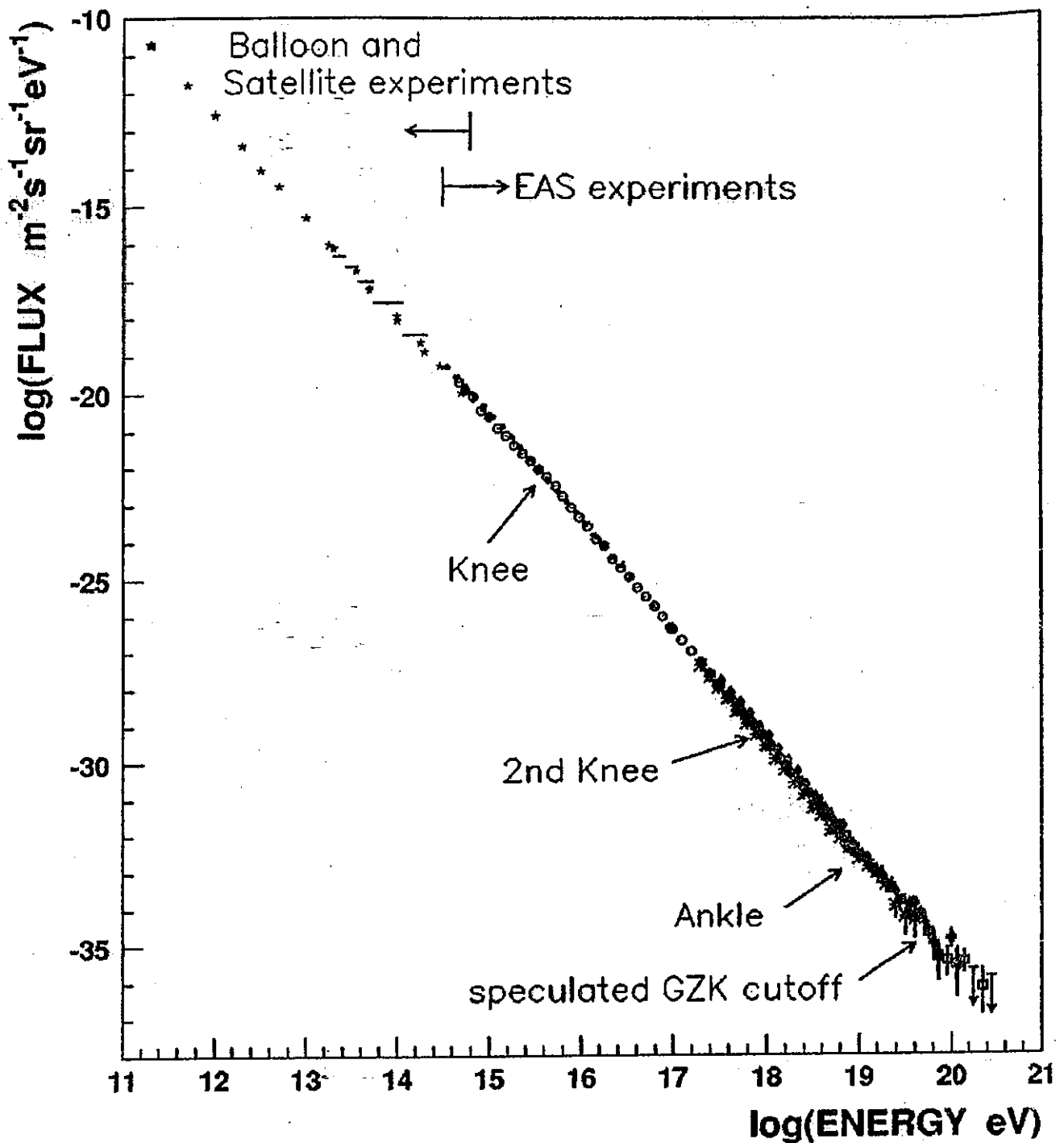


FIG. 1. Observed energy spectrum of primary cosmic rays. The spectrum is expressed by a power law from 10^{11} to 10^{20} eV with a slight change of slopes around $10^{15.5}$ eV (knee), $10^{17.8}$ eV (second knee), and 10^{19} eV (ankle). The integral fluxes above the “knee” and the “ankle” are approximately 1 per m^2 year and 1 per km^2 year. Details of the spectrum and sources of the data above 10^{17} eV are shown in Figs. 23 and 24.

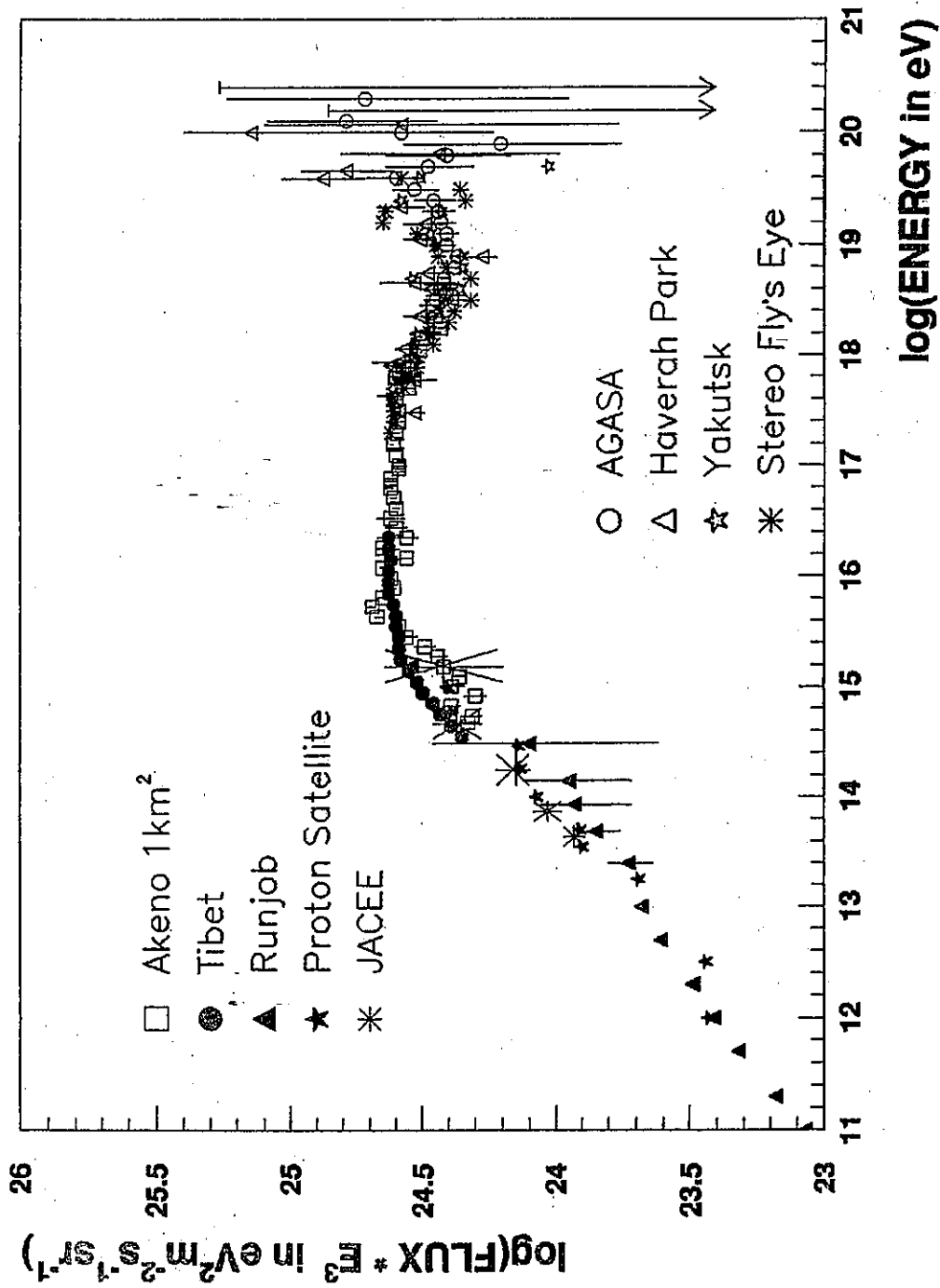


FIG. 24. Differential energy spectrum of primary cosmic rays over a broad energy range. Plots above 10¹⁸ eV are from four experiments (Haverah Park, Yakutsk, Fly's Eye, AGASA) and open squares are data from the Akeno 1-km² array. Other signals below 10¹⁶ eV are from Tibet at mountain altitude (Amenomori *et al.*, 1996a), direct measurements taken from balloons, JACEE (Asakimori *et al.*, 1993) and RUNJOB (Ichimura *et al.*, 1993), and the Proton Satellite (Grigorov *et al.*, 1971).

1. 序論

エネルギー・スペクトル

・ べき型 $N(E) \propto E^{-\alpha}$

・ 折れ曲がり knee
ankle

エネルギー・密度

$\sim 1 \text{ eV cm}^{-3}$ at GeV

$\sim 10^{-4} \text{ eV cm}^{-3}$ knee

$\sim 10^{-8} \text{ eV cm}^{-3}$ ankle

$\sim 10^{-9} \text{ eV cm}^{-3}$ 10^{20} eV

組成

p, He, C, O, ..., Fe, ...

(spallation $p + (C, O) \rightarrow \text{Li, Be, B}$)

(unstable isotope $^{10}\text{Be} \rightarrow ^{10}\text{B}$)

GLACK:

OFFENDING COMMAND:

ERROR: undefined

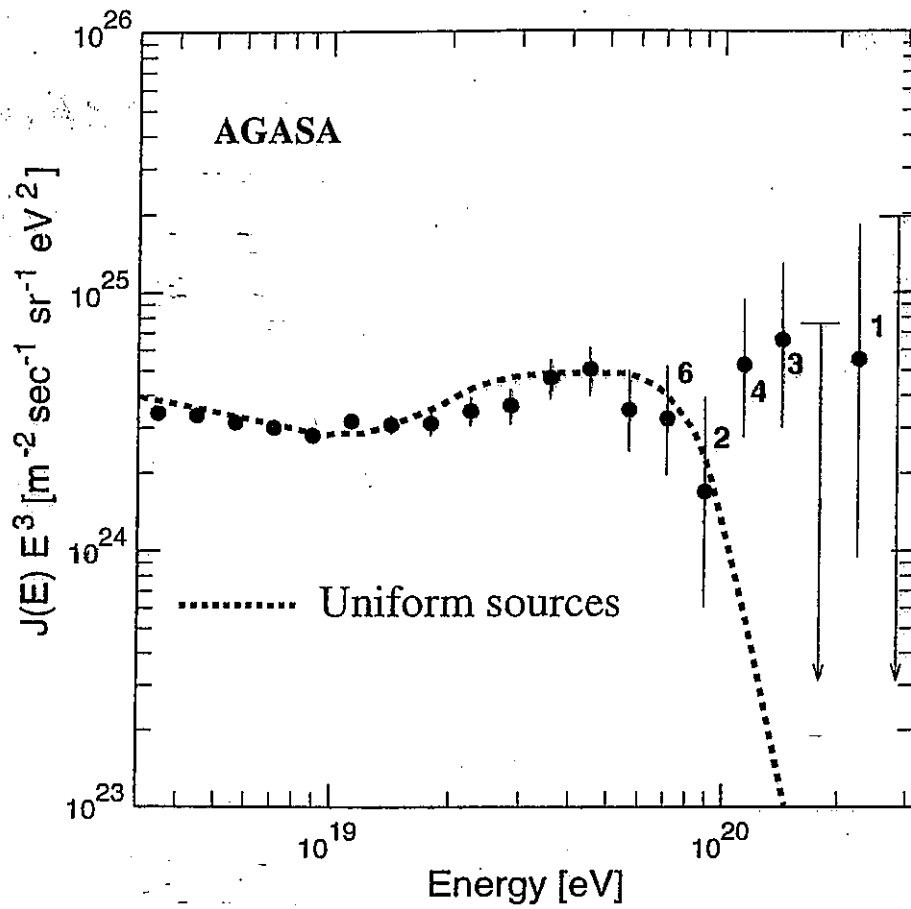
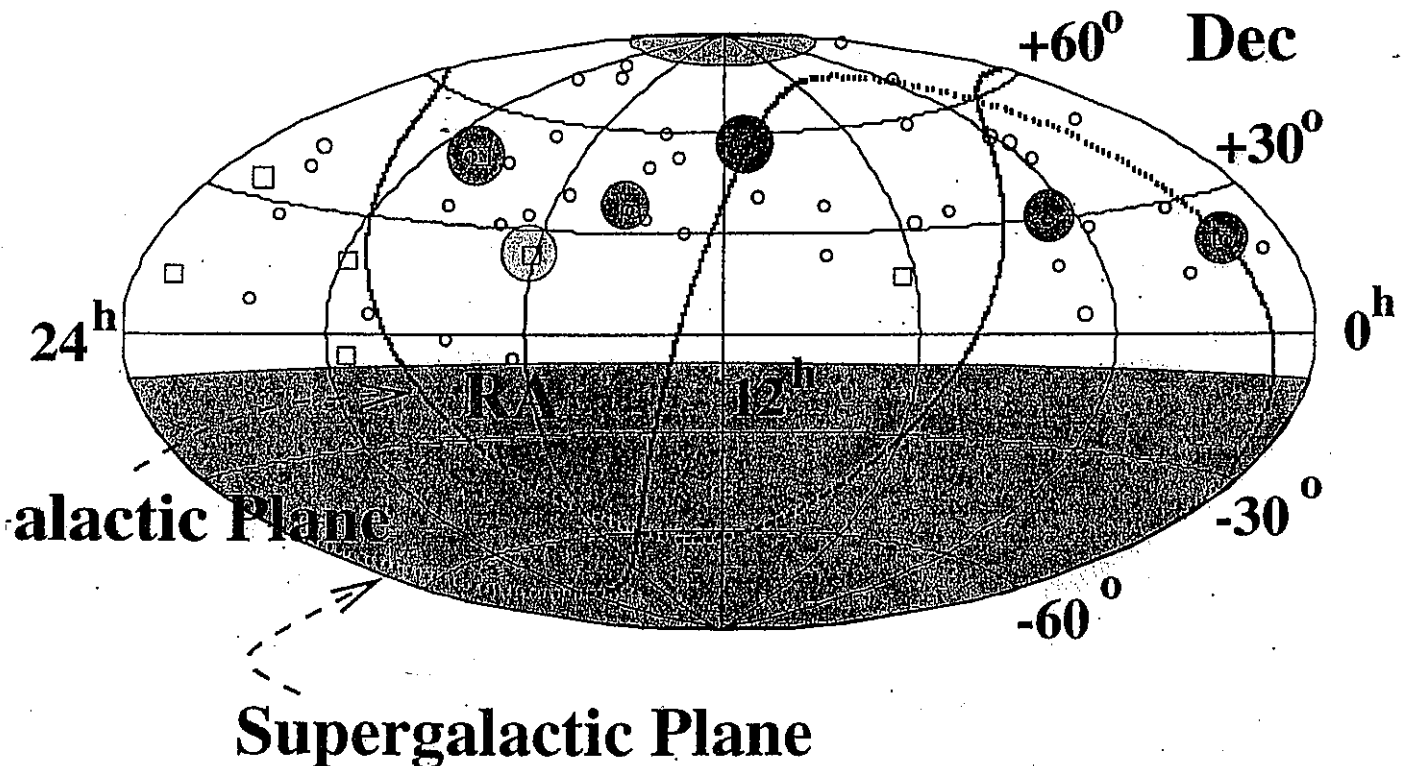
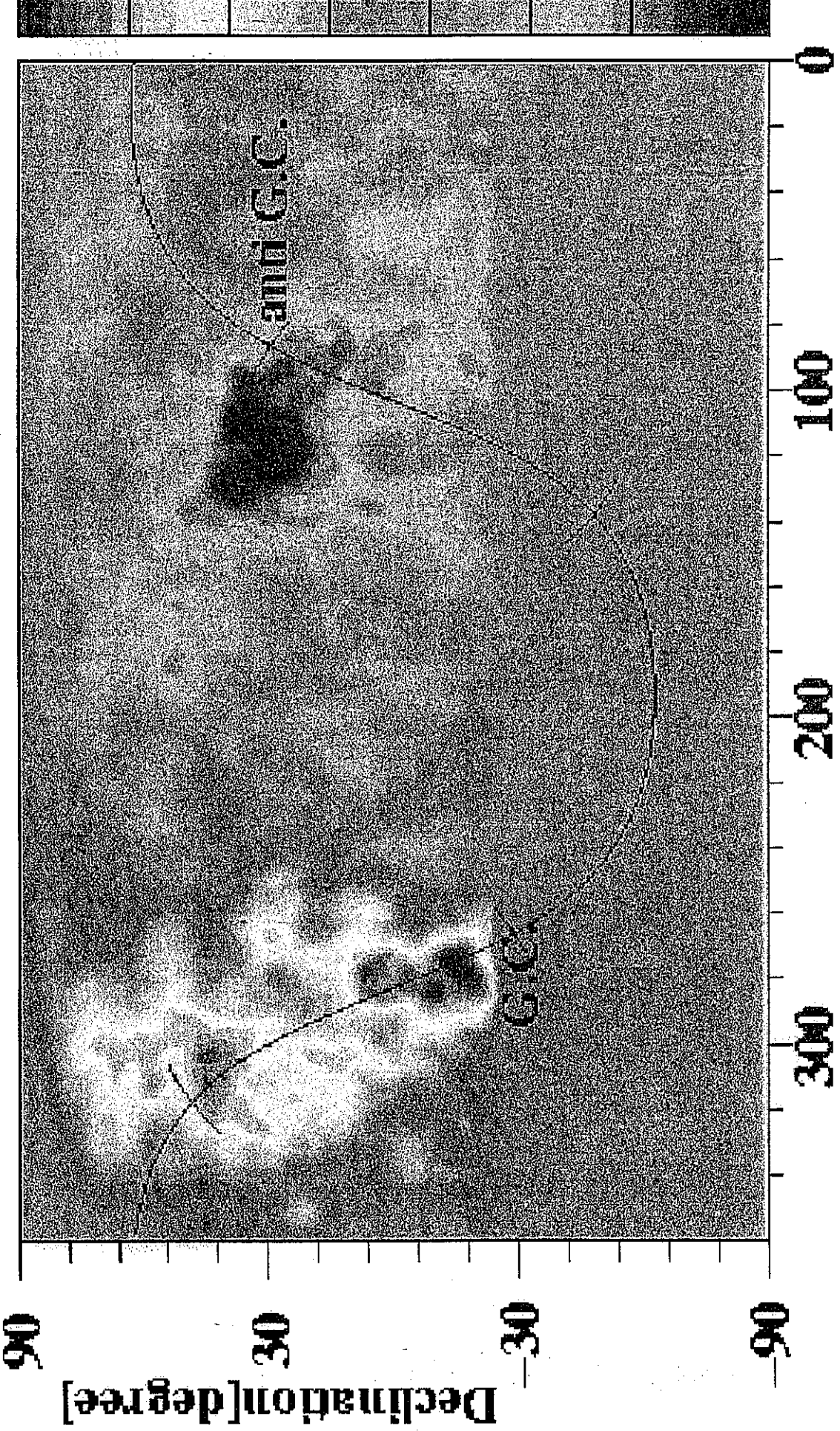


Fig. 1. The energy spectrum observed by AGASA. The vertical axis is multiplied by E^3 . Error bars represent the Poisson upper and lower limits at 68% and arrows are 90% C.L. upper limits. Numbers attached to points show the number of events in each energy bin. The dashed curve represents the spectrum expected for extragalactic sources distributed uniformly in the Universe, taking account of the energy determination error. The primary spectrum is assumed $\propto E^{-2.3}$.

AGASA + A20



4 3 2 1 0 -1 -2 -3



Right Ascension [degree]

Declination [degree]

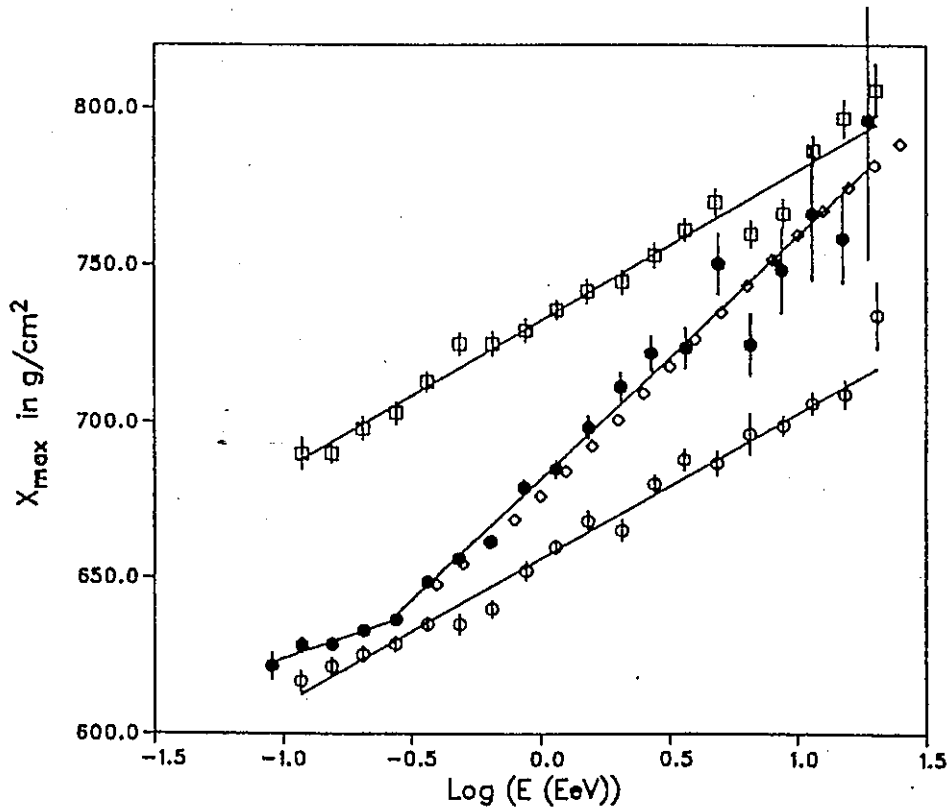
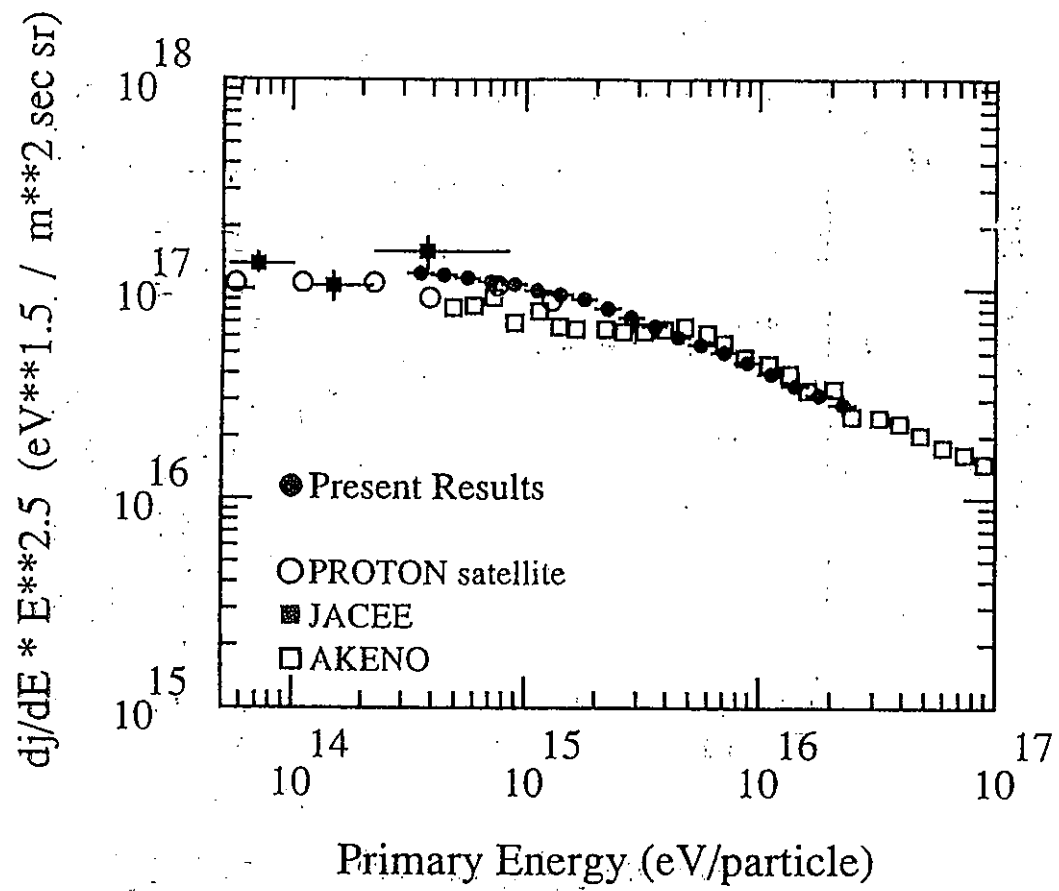
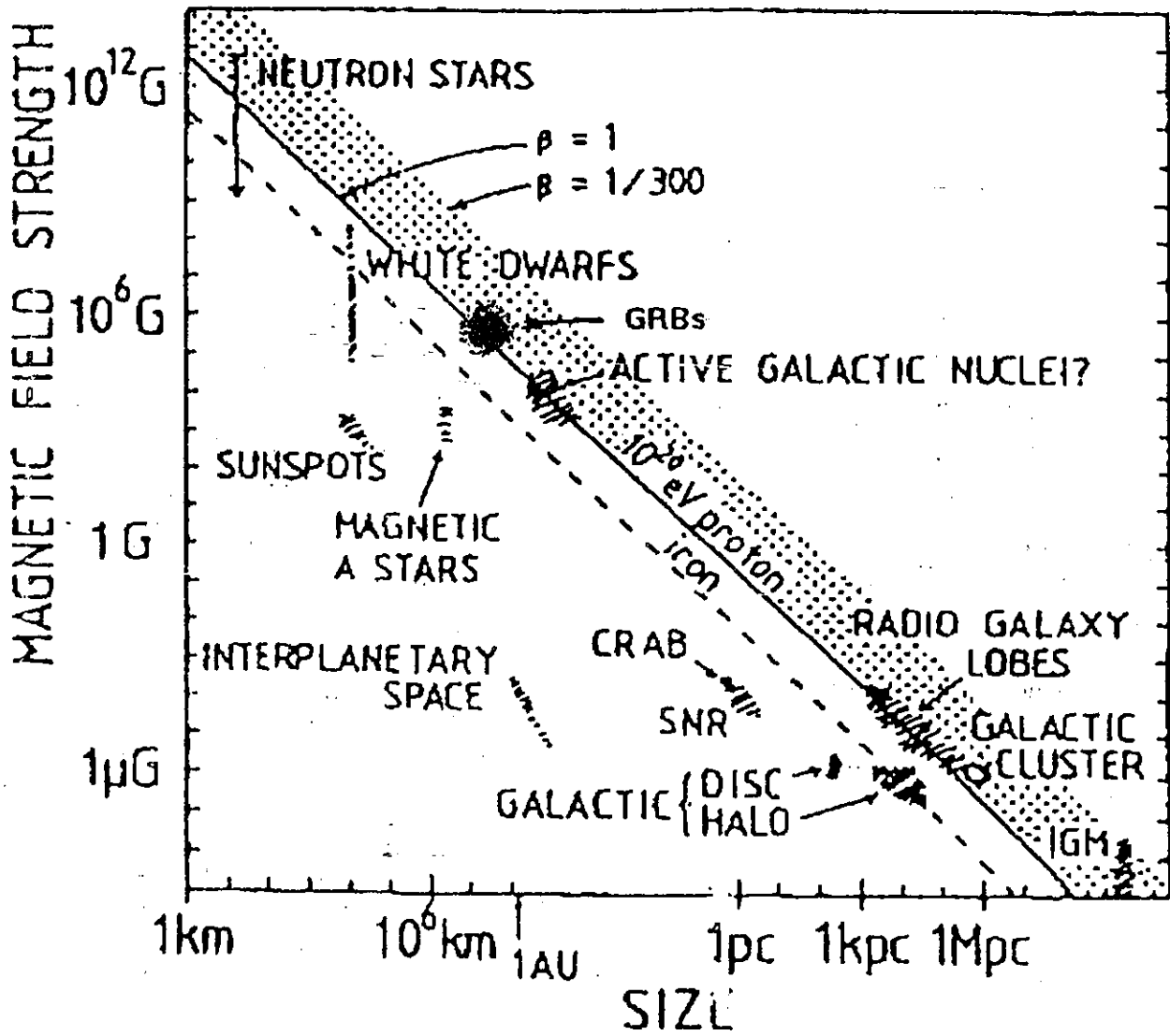
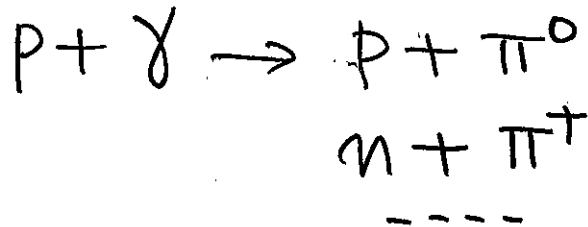


FIG. 3. X_{\max} elongation rate are plotted against $\log_{10} E$. Black dots: Fly's Eye data. Open squares: proton X_{\max} distribution based on QCD Pomeron model. Open circles: iron X_{\max} distribution based on QCD Pomeron model. Diamonds: expected mean X_{\max} distribution based on a simple two-component assumption of cosmic rays.



Above the ankle

• GZK cutoff



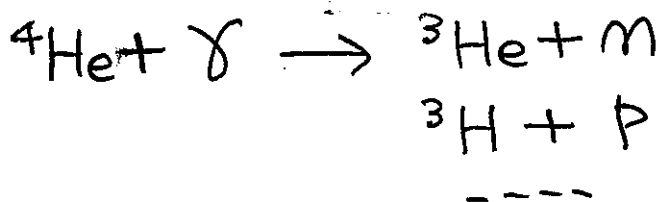
threshold $E_p E_\gamma = \frac{m_p m_\pi}{2}$

$$E_\gamma \sim \text{meV}$$

$$\underline{\underline{E_p \sim 6 \times 10^{19} \text{ eV}}}$$

$$\underline{\underline{\Omega \sim \frac{1}{n_\gamma \sigma} \sim 10 \text{ Mpc}}}$$

• 原子核の光分解



(Giant Dipole Resonance)

$$E_{\text{tr}} \sim 20 \text{ MeV}$$

$$\text{meV} \times \frac{10^{20} \text{ eV}}{4 \text{ GeV}} \sim 25 \text{ MeV}$$

Fe, C, O 等とも同様

CMB, CIB 等がきく

I. Observational requirements

- * spectrum continuation up to $\sim 10^{20.5} \text{ eV}$
($d \lesssim 25-100 \text{ Mpc}$)
- * composition proton dominance?
- * anisotropy basically isotropic

deflection angle

$$\theta \sim \sqrt{\frac{d}{\lambda}} \frac{\lambda}{R_L} \sim \frac{10^{20} \text{ eV}}{E} \cdot \frac{B}{10^{-9} \text{ G}} \frac{\sqrt{d\lambda}}{10^2 \text{ Mpc}}$$

d : source distance

λ : coherence length of B

If clustering is real, $\theta \ll 1$ and

$$\underline{n \sim 6 \times 10^{-3} \text{ Mpc}^{-3}} \quad (\text{Dubovskiy et al. 2000})$$

$\sim n$ (bright galaxies)

* energetics $U (> 10^{19} \text{ eV}) \sim 10^{-20} \text{ erg cm}^{-3}$

$U (> 10^{20} \text{ eV}) \sim 10^{-21} \text{ erg cm}^{-3}$

$n L_{\text{CR}} \tau \sim U$

$E > 10^{19} \text{ eV}, \tau \sim 10^{17} \text{ sec}$

$\Rightarrow \frac{n}{\text{Mpc}^3} \cdot \frac{L_{\text{CR}}}{10^{45} \text{ erg/s}} \approx 10^{-8.5}$

$E > 10^{20} \text{ eV}, \tau \sim 10^{15.5} \text{ sec}$

$\Rightarrow \frac{n}{\text{Mpc}^3} \cdot \frac{L_{\text{CR}}}{10^{45} \text{ erg/s}} \approx 10^{-8}$

source spectrum of EHECR

must be very hard.

harder than $N(E) \propto E^{-1.5}$

incompatible with observation

\Rightarrow two-component $\left\{ \begin{array}{l} \text{galactic at } E < E_*? \\ \text{extragalactic at } E > E_*? \end{array} \right.$

$E_* \sim 10^{19.5} \text{ eV}$

E^{-3}

E^{-1}

II. Possible acceleration processes

Confinement and Modulation

$$* R_L = \frac{E}{qB} < R$$

$$\text{for } E=10^{20} \text{ eV}, \quad BR > 0.1 \text{ G} \cdot \text{pc}$$

* electro-static potential

$$q \Delta \Phi \approx q \frac{V}{c} B R \approx 10^{21} \text{ eV} \left(\frac{V}{c} \right) \cdot \frac{B}{\text{G}} \frac{R}{\text{pc}}$$

ex.

Earth magnetosphere

$$B \sim 1 \text{ G}, \quad R \sim 10^{-10} \text{ pc} \quad \Rightarrow \quad E_L \sim 10^{11} \text{ eV}$$

geo-magnetic cutoff

Heliosphere

$$B \sim 10^{-5} \text{ G}, \quad R \sim 10^{-5} \text{ pc} \quad \Rightarrow \quad E_L \sim 10^{11} \text{ eV}$$

modulation of
galactic cosmic rays

$$\frac{V}{c} \sim 10^{-3} \quad \Rightarrow \quad q \Delta \Phi \sim 10^8 \text{ eV}$$

acceleration of anomalous
cosmic rays

Galaxy

$$B \sim 10^{-5} \text{ G}, R \sim 10^{3-4} \text{ pc} \Rightarrow E_L \sim 10^{19-20} \text{ eV}$$

modulation of extra-galactic
cosmic rays?

$$\frac{V}{c} \sim 10^{-3}$$

$$\Rightarrow q \Delta \Phi \sim 10^{16-17} \text{ eV}$$

between the knee and ankle?

Radio galaxies

hot spots $B \sim 10^{-3} \text{ G}, R \sim 10^3 \text{ pc} \Rightarrow E_L \sim 10^{21} \text{ eV}$

cocoons $\frac{V}{c} \sim 10^{-1}$

$$q \Delta \Phi \sim 10^{20} \text{ eV}$$

$$B \sim 10^{-4} \text{ G}, R \sim 10^5 \text{ pc} \Rightarrow E_L \sim 10^{22} \text{ eV}$$

$$\frac{V}{c} ?$$

Clusters of galaxies

$$B \sim 10^{-7} \text{ G}, R \sim 10^6 \text{ pc} \Rightarrow E_L \sim 10^{20} \text{ eV}$$

$$\frac{V}{c} \sim 10^{-2}$$

$$q \Delta \Phi \sim 10^{18} \text{ eV}$$

GRB

$$B \sim 10^2 \text{ G}, R \sim 10^{-2} \text{ pc} \Rightarrow E_L \sim 10^{21} \text{ eV}$$

$$\frac{V}{c} \sim 1$$

(relativistic shock)

$$q \Delta \Phi \sim 10^{21} \text{ eV}$$

	加速	光度	等方性
Radio Galaxies	○	○	△

$$n_{RG} \sim 10^{-5} \text{ Mpc}^{-3}$$

$$L_{CR} \sim 10^{42} \text{ erg s}^{-1}$$

* FR II vs FR I

GRB	△	○	△
-----	---	---	---

$$\dot{n}_{GRB} \sim 1 \text{ day}^{-1} \cdot \text{Gpc}^{-3} \sim 10^{-14} \text{ s}^{-1} \cdot \text{Mpc}^{-3}$$

$$E_{GRB} \sim 10^{51} \text{ erg}$$

$$\dot{n}_E \sim 10^{37} \text{ erg s}^{-1} \text{ Mpc}^{-3}$$

* 到達時間 $\tau \sim \theta^2 \frac{d}{c} \sim \theta^2 \times 10^8 \text{ yr} \frac{d}{30 \text{ Mpc}}$

Clusters of Galaxies

?	○	△
---	---	---

* 加速時間 \sim 宇宙時間

源からの GZK cutoff

Normal Galaxies

?

○

○

* our Galaxy には 何故 $\sim 10^{18-19} \text{ eV}$ までの粒子を
加速できるのか?

(Massive Black Holes
Radiatively Quiescent)

?

?

?

Close this window to return to the previous window

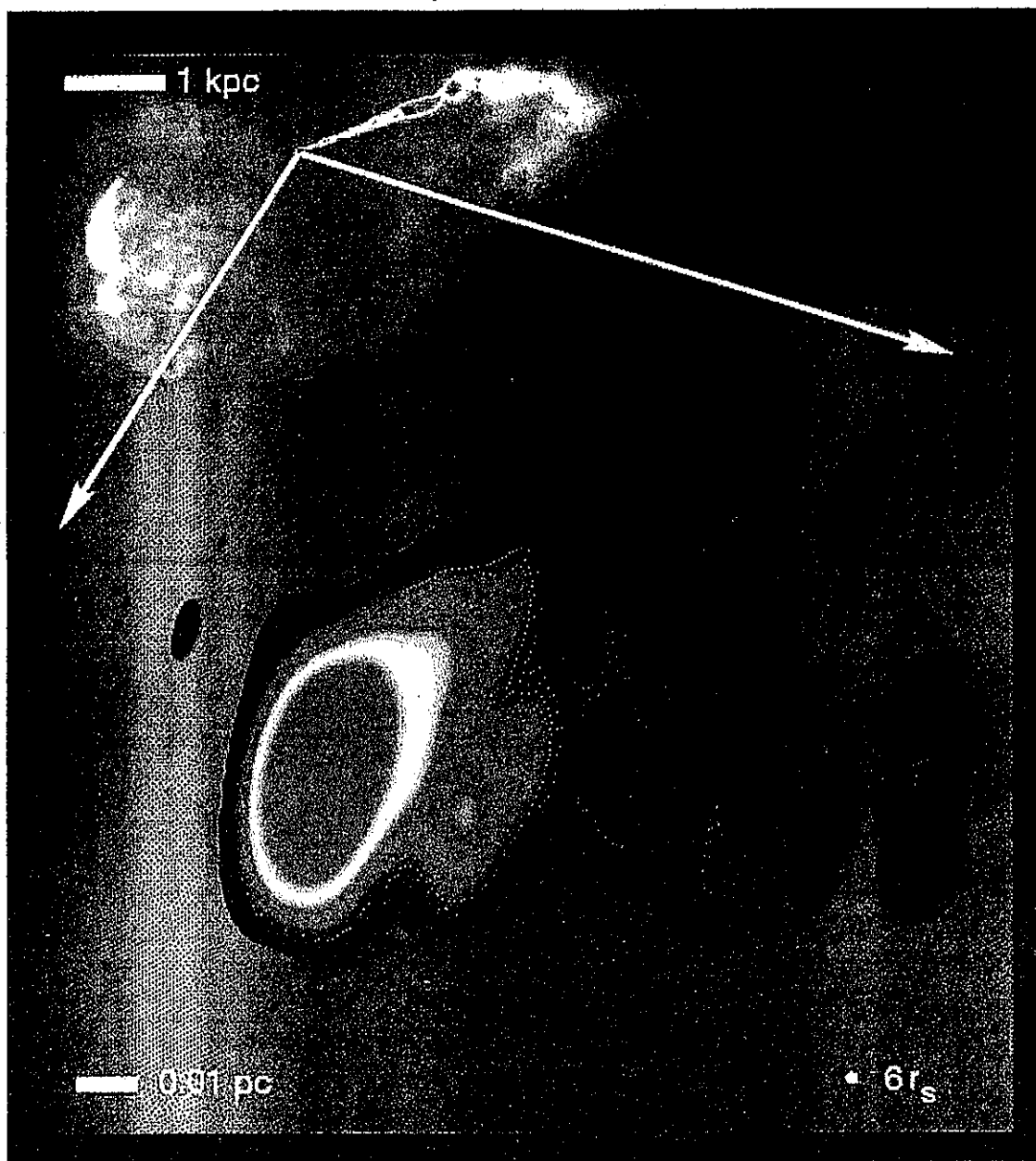


Figure 2 Pseudo-colour rendition of the nucleus of M87 at 43 GHz on 3 March 1999. See Fig. 1 for details. The filled white circle at lower right indicates $6r_s$, which is the diameter of the last stable orbit around a non-rotating black hole. The inset (top left) is a 15-GHz VLA image illustrating the large-scale jet.

← item →

Note: Figures may be difficult to render in a web browser. In such cases, we recommend downloading the PDF version of this document.

Cygnus A

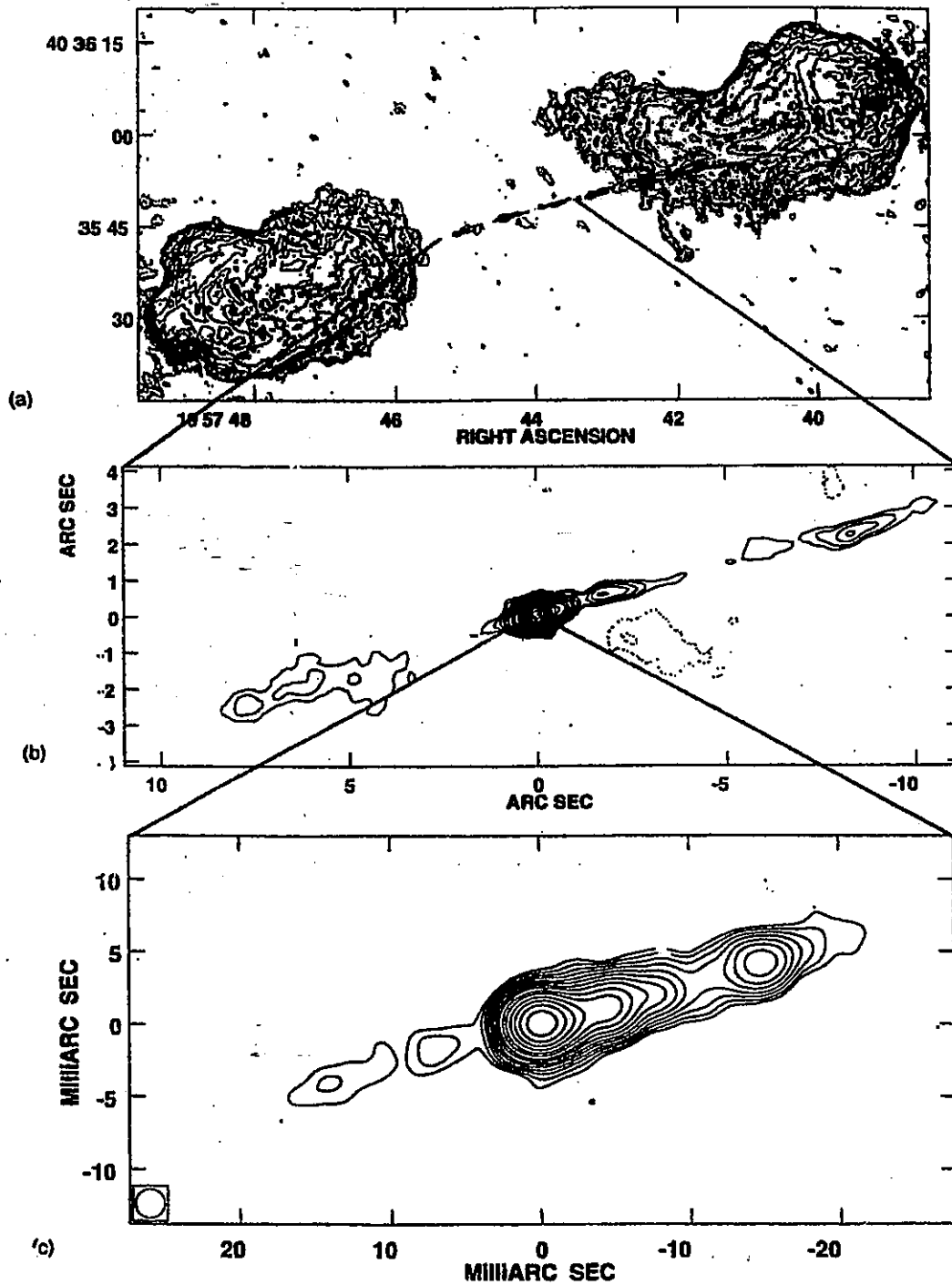


FIG. 4. Contour images of the Cygnus A radio jet on various scales, reproduced from Carilli *et al.* (Ref. 65). The top image shows the kpc-scale radio source at 5 GHz with a resolution of 0.4 arc sec. The contour levels are a geometric progression in \sqrt{I} , which implies a factor of 2 rise in surface brightness every two contours. The middle image is of the inner kpc-scale jet of Cygnus A with the same contouring as above. The bottom image shows the pc-scale jet of Cygnus A at 3mas resolution (FWHM).

Phys. Plasmas, Vol. 5, No. 5, May 1998

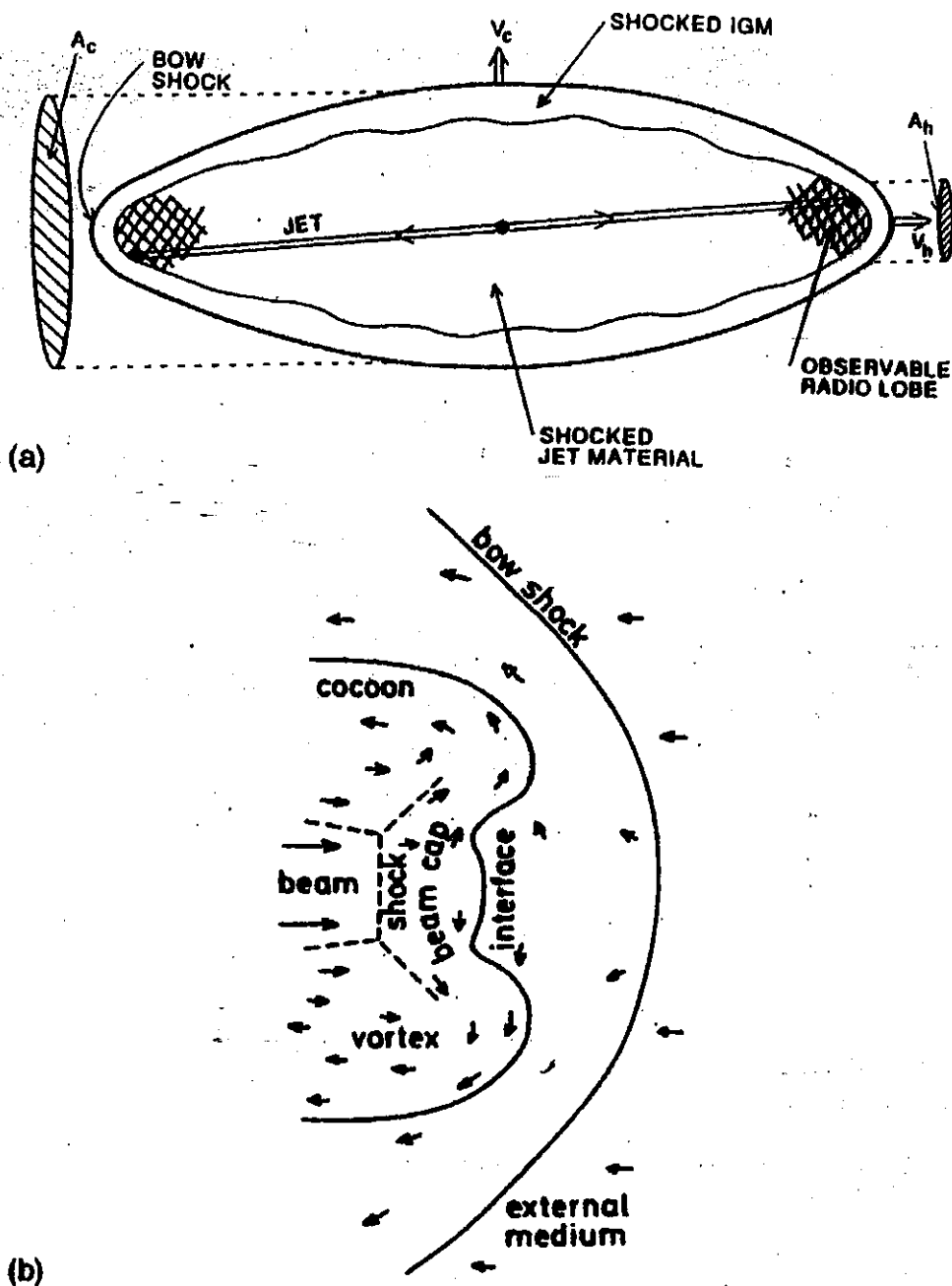
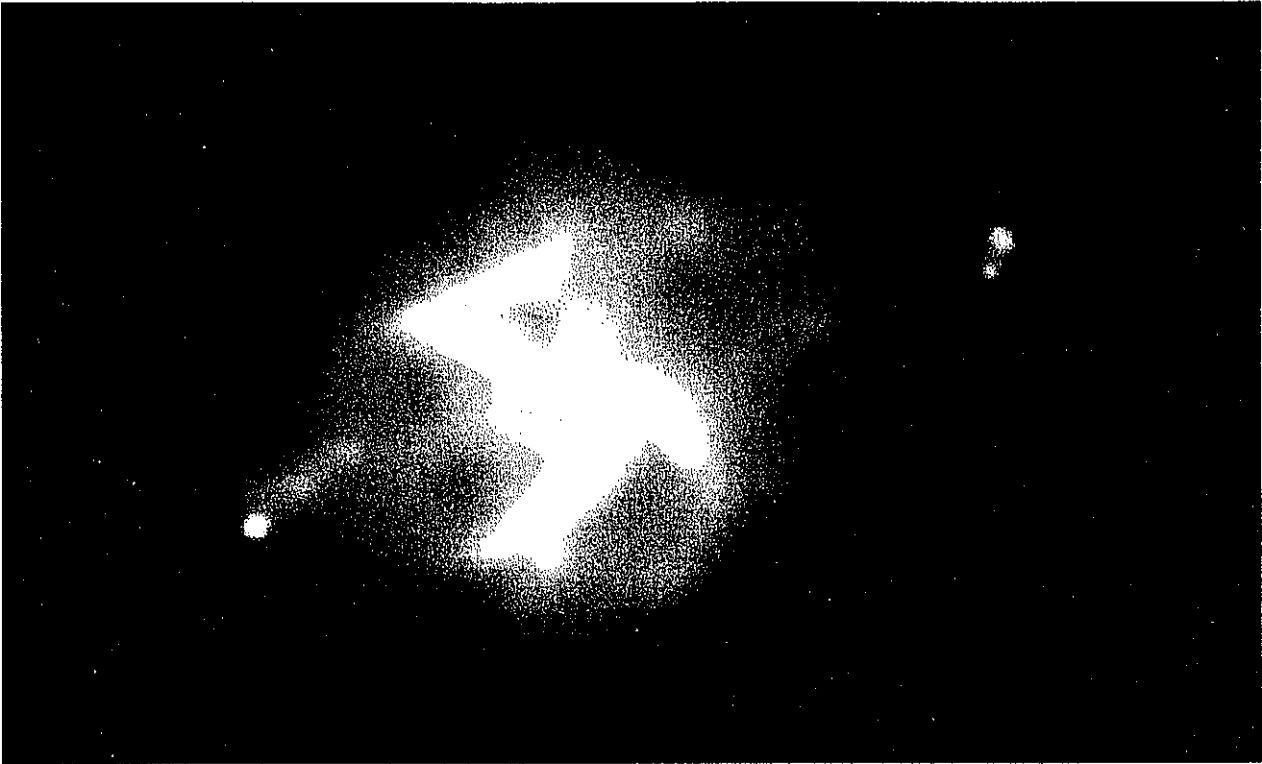


FIG. 3. A schematic representation showing the effect an expanding radio source will have on the external medium. (a) is reproduced from Begelman and Cioffi (Ref. 63), and shows the expected large-scale distribution of shocked ambient gas enveloping the radio lobes. (b) is reproduced from Smith *et al.* (Ref. 64) and shows a detail of the expected double-shock structure at the jet terminus. The interface is the contact discontinuity between shocked jet material and shocked intracluster material (ICM). The beam shock and cap correspond to the radio hotspots, and the cocoon corresponds to the radio lobe.

ERROR: undefined
OFFENDING COMMAND:

STACK:



**Chandra X-Ray
Observatory Center**

Harvard-Smithsonian Center for Astrophysics
60 Garden Street, Cambridge, MA 02138
<http://chandra.harvard.edu>

Cygnus A: A galaxy, some 700 million light years away, with a central black hole.
Credit: NASA/UMD/A. Wilson et al.

Chandra's image shows a giant football-shaped cavity within X-ray emitting hot gas surrounding the galaxy Cygnus A. The cavity in the hot gas has been created by two powerful jets emitted from the central black hole region. The jets themselves terminate in radio and X-ray emitting "hot spots," some 300,000 light years from the center of the galaxy. Scientists believe that fast atomic particles and magnetic fields from the jets spill out into the region, providing pressure that continuously inflates the cavity.

Scale: Image is 3.3 x 2 arcmin.

Chandra X-ray Observatory ACIS image

1/13/97

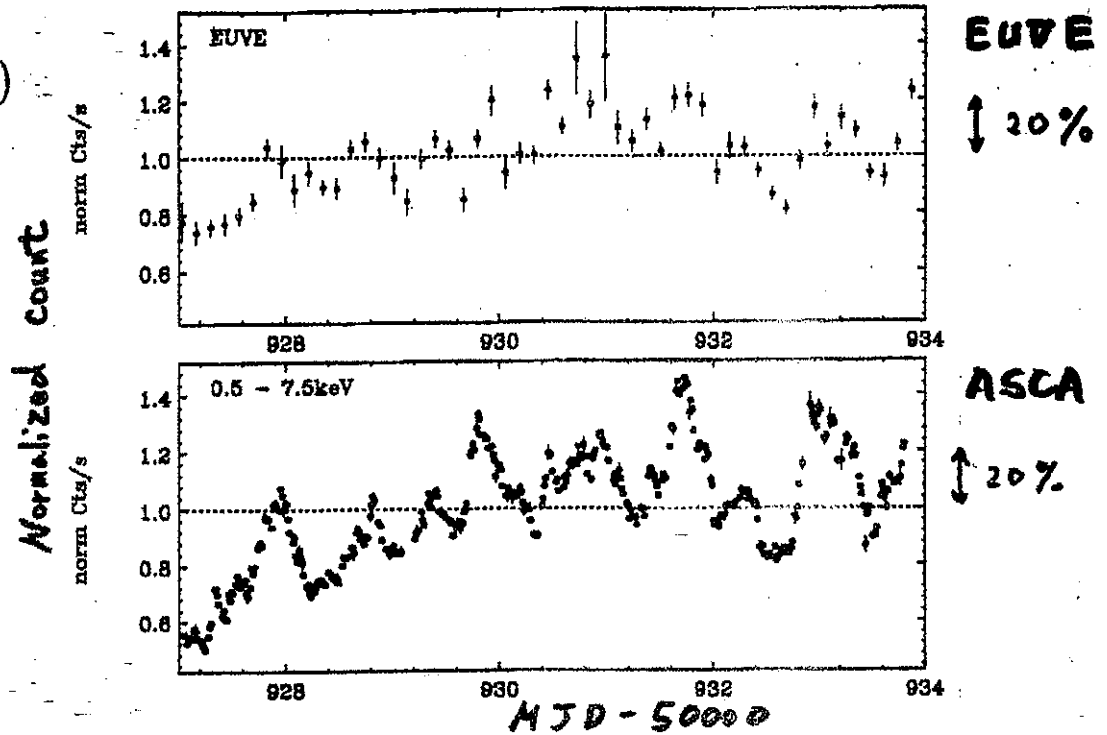
Two big campaigns of TeV blazars

- 7 days continuous observation of Mrk 421

(PI: T.Takahashi)

1998 Apr

EUVE
ASCA

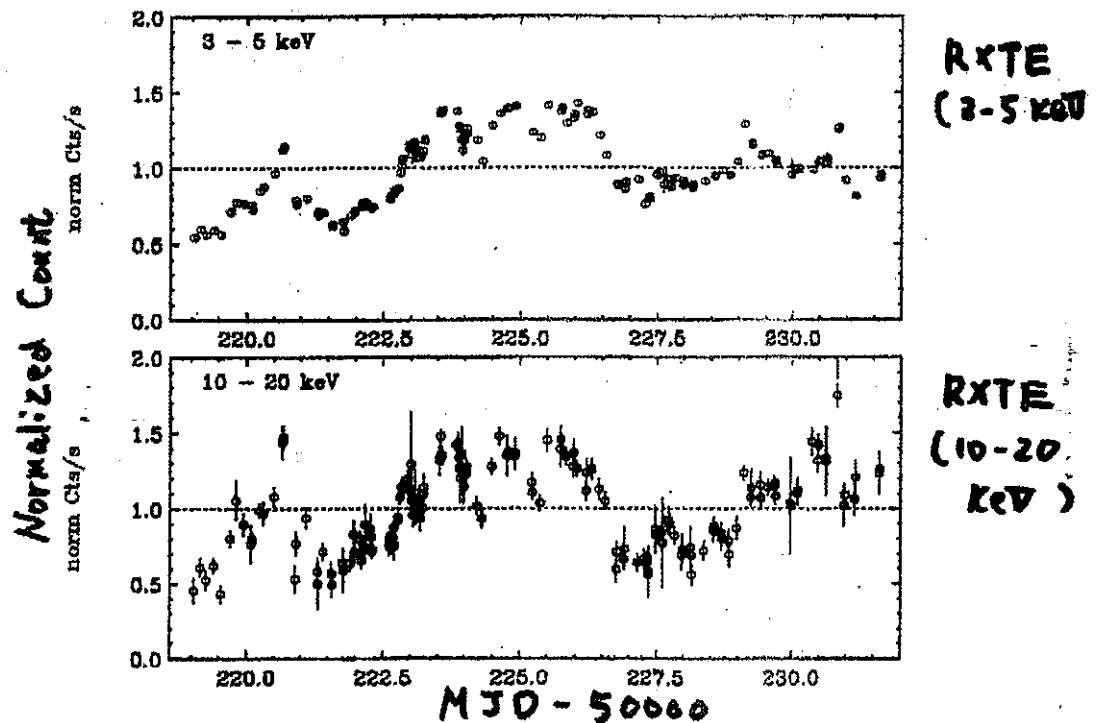


- 12 days continuous observation of PKS2155-304

(PI: C.M.Urry)

1996 May

RXTE

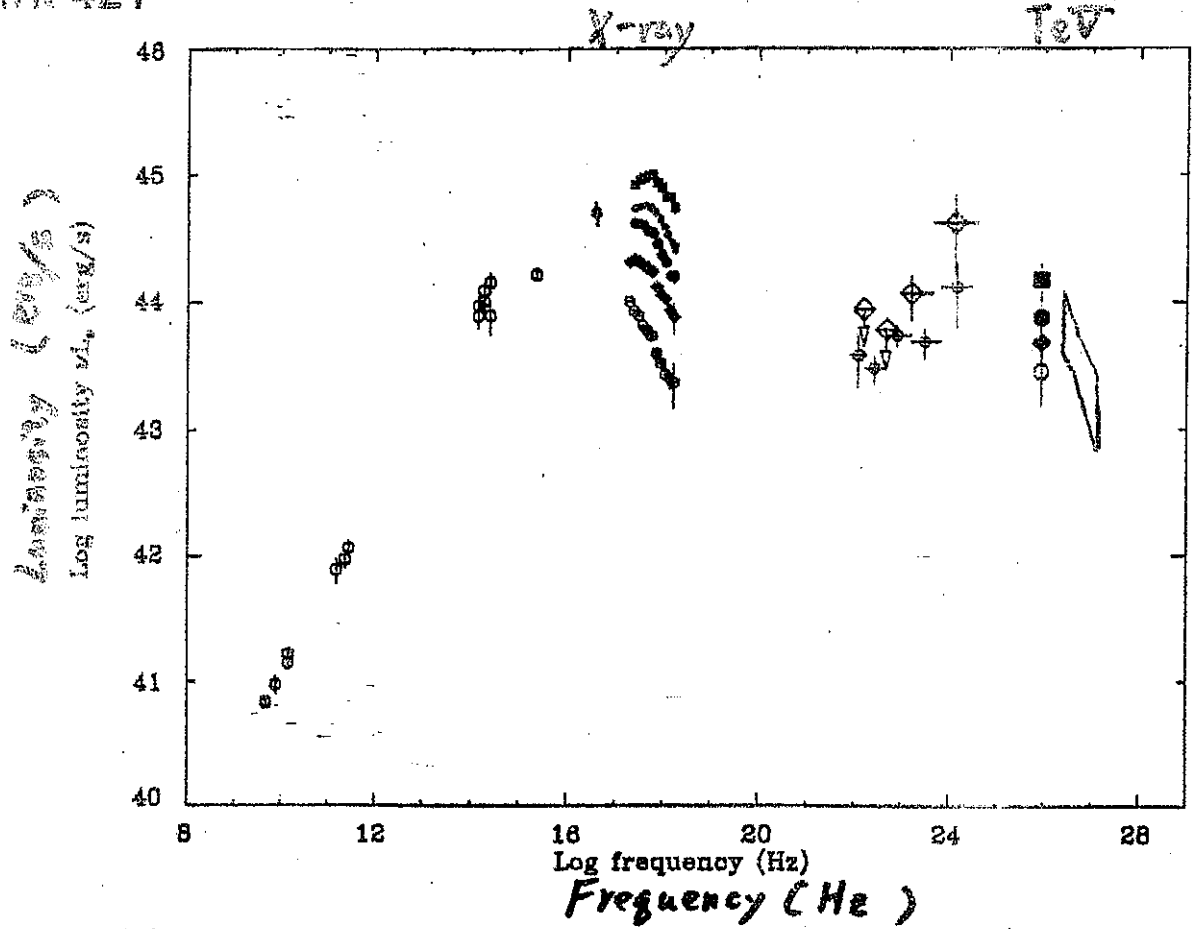


- (1) Light curves include ~ 10 day-by-day flares
- (2) Amplitude of variation becomes larger at higher energy band
- (3) Many of flare events have symmetric time profiles

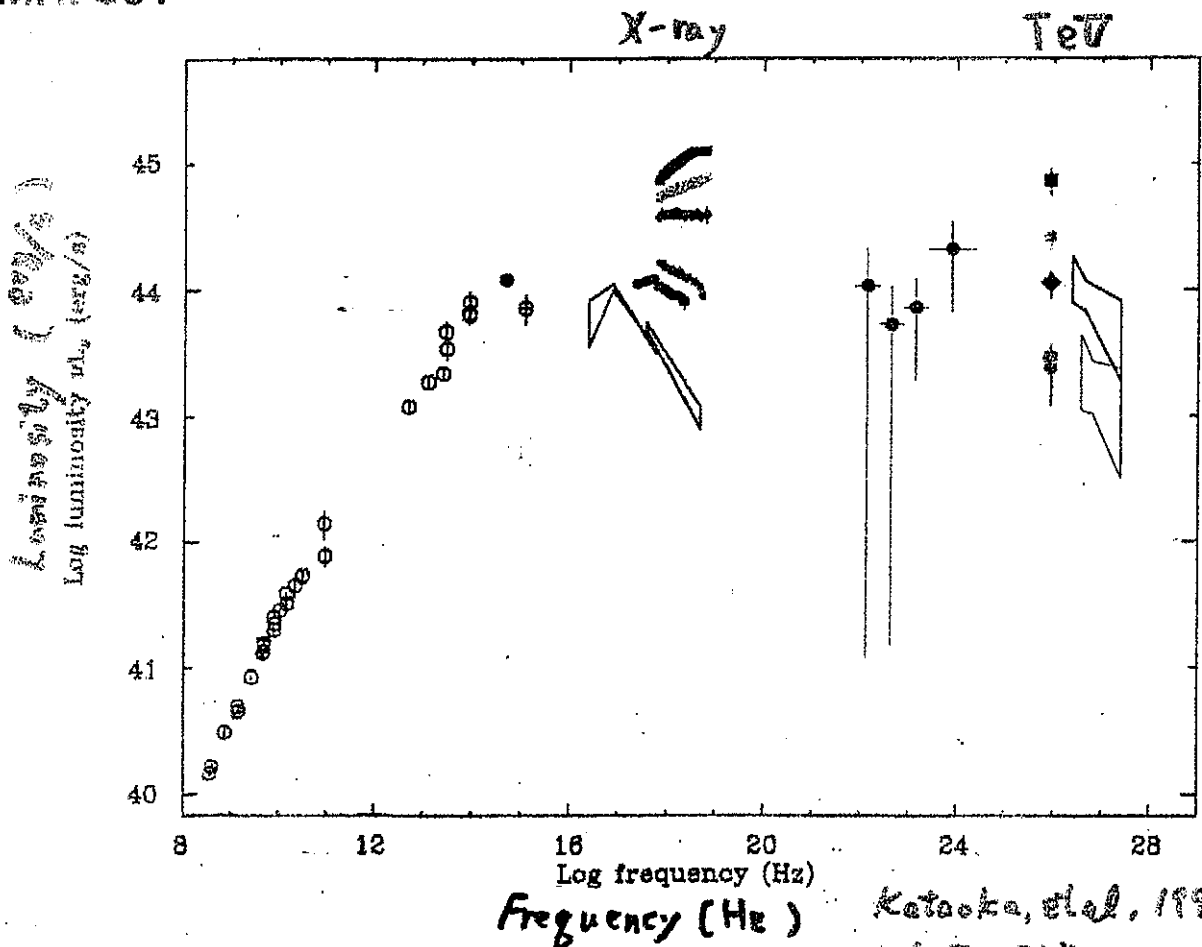
片岡

Evolution of the Multifrequency Spectra

(1) Mrk 421



(2) Mrk 501



Kataoka, et al., 1999

ApJ, 517

Relativistic Beaming

- superluminal expansion ($v_{app} \sim 10c$)
- rapid time variability ($\Delta t \sim 10^3 - 10^5 s$)
- high polarization
- featureless continuum dominated

**Synchrotron
radiation**

relativistic boosted emission from jets
dominates over thermal components

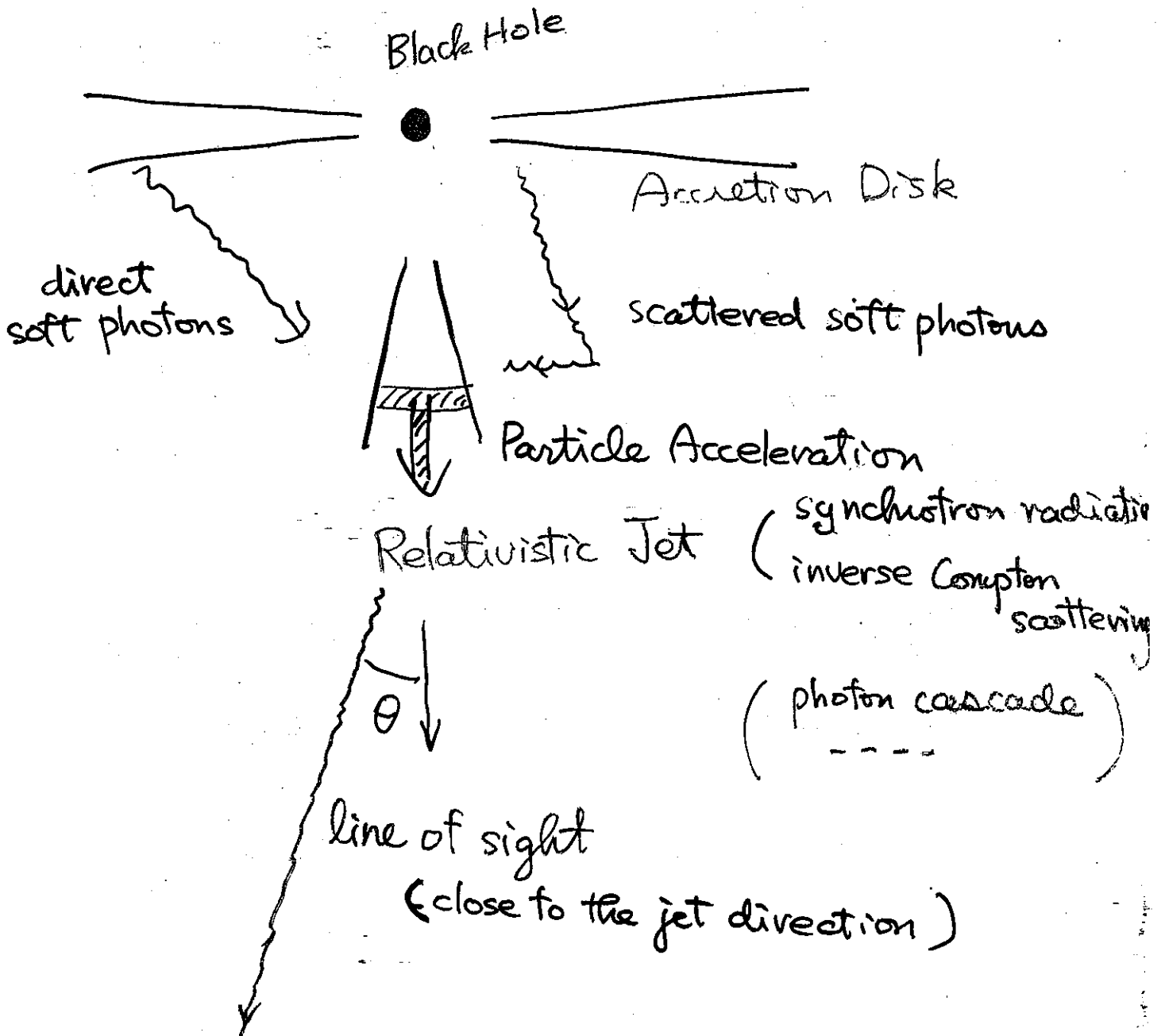
- GeV - TeV γ -rays

**inverse Compton
scattering**

no evidence for internal γ - γ absorption
also means relativistic beaming

$$\Gamma \sim 10 \quad , \quad R \sim 10^{-2} \text{ pc} \sim 10^2 r_g$$

Model Ingredients



beaming factor

$$\delta \equiv \frac{1}{\Gamma(1 - \beta \cos \theta)}$$

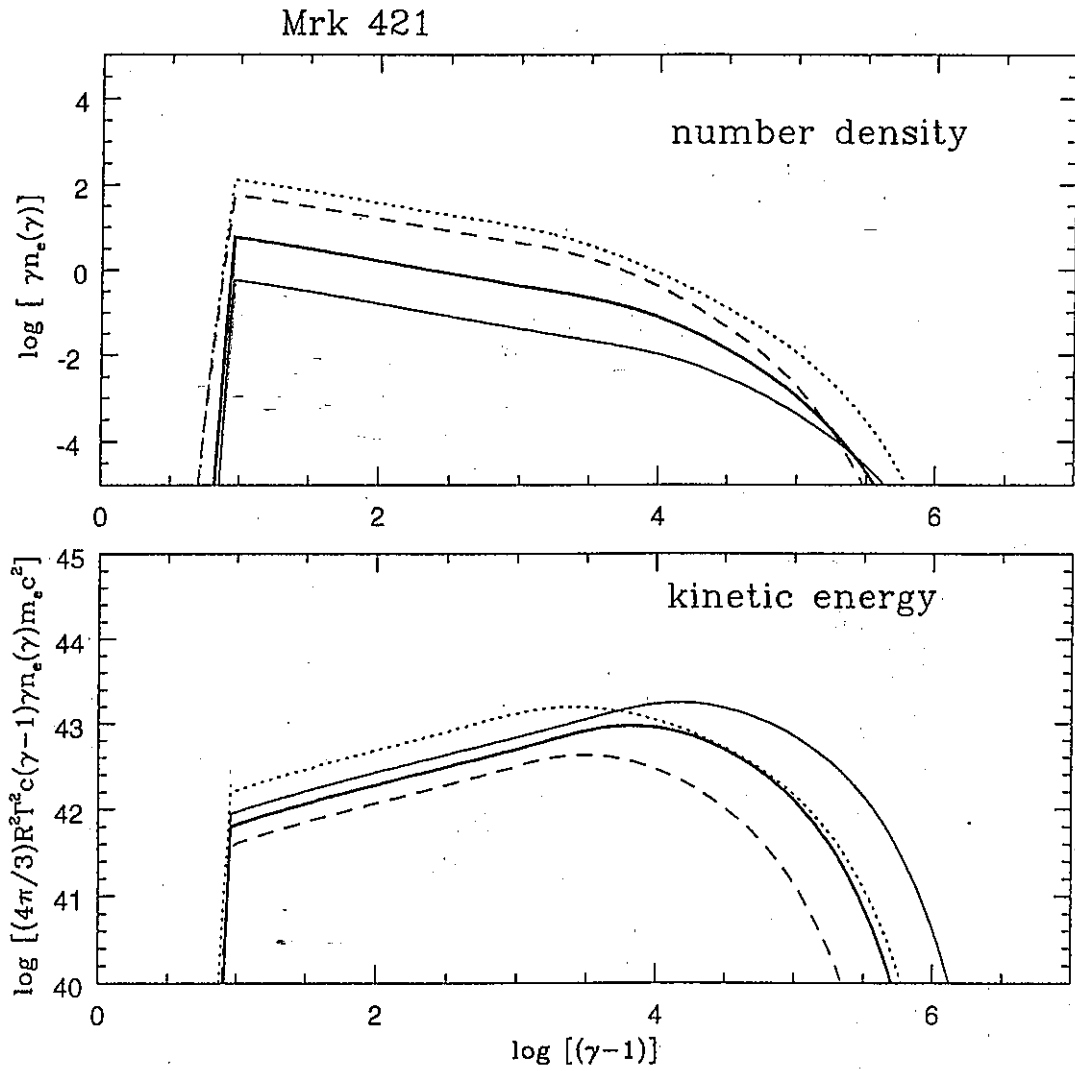


Fig. 5.— Electron energy spectrum and kinetic power of Mrk 421 corresponding to Figure 4.

$$\frac{u_e}{u_B} = 11$$

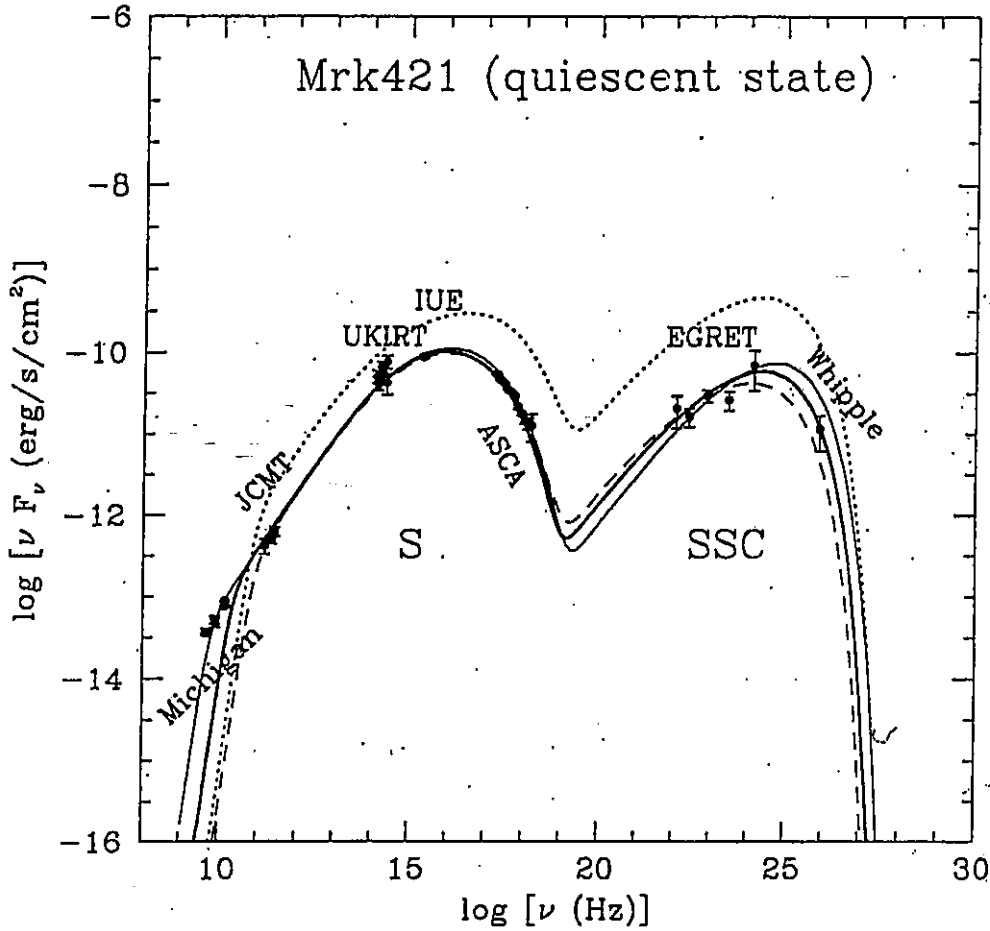


Fig. 4.— One-zone SSC model spectra for the steady state emission of Mrk 421. Thick solid line shows the best fit spectrum, where adopted parameters are $\delta = 12$, $R = 2.8 \times 10^{16}$ cm, $B = 0.12$ G, $\gamma_{\max} = 1.5 \times 10^5$, $q_e = 4.1 \times 10^{-6}$ cm $^{-3}$ s $^{-1}$, $s = 1.6$, and $u_e/u_B = 11$. Dotted line shows the spectrum obtained using the analytic estimates for Mrk 421. Thin solid and dashed lines show the spectra of low and high injection models, respectively, to indicate the uncertainty range of the spectral fitting.

* γ_{\max} cooling limited

$$\tau_{\text{acc}} = \frac{3}{V_1 - V_2} \left(\frac{K_1}{V_1} + \frac{K_2}{V_2} \right) \quad \text{for standard non-relativistic shocks}$$

Various complications for relativistic shocks
 obliqueness, non-diffusive return for upstream
 Böhm diffusion for downstream

guess $V_2 = \frac{V_1}{3}$, $K_2 = \frac{V_1 C}{3}$, $K_1 = 0$

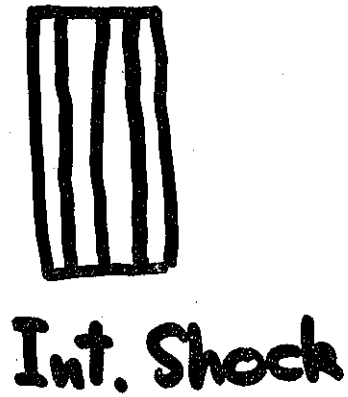
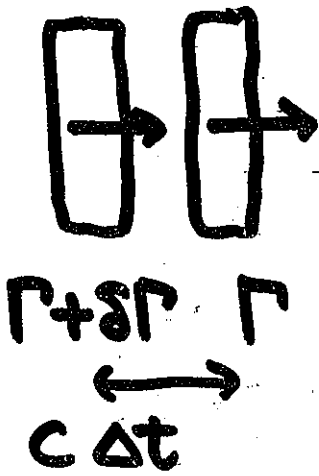
$$\tau_{\text{acc}} = \frac{9}{2} \frac{V_3}{C} \quad V_3 = \frac{\gamma_{\text{mec}^2}}{eB}$$

$$\tau_{\text{acc}} = \tau_{\text{cool}}$$

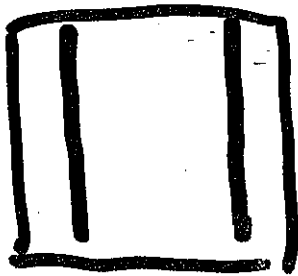
$$\gamma_{\max} = 1.1 \times 10^7 \left(\frac{B}{U_{\text{soft}}} \right)^{1/2} \Rightarrow \text{correct tendency of higher } \gamma_{\max} \text{ for less luminous sources}$$

If γ_{\max} is escape limited

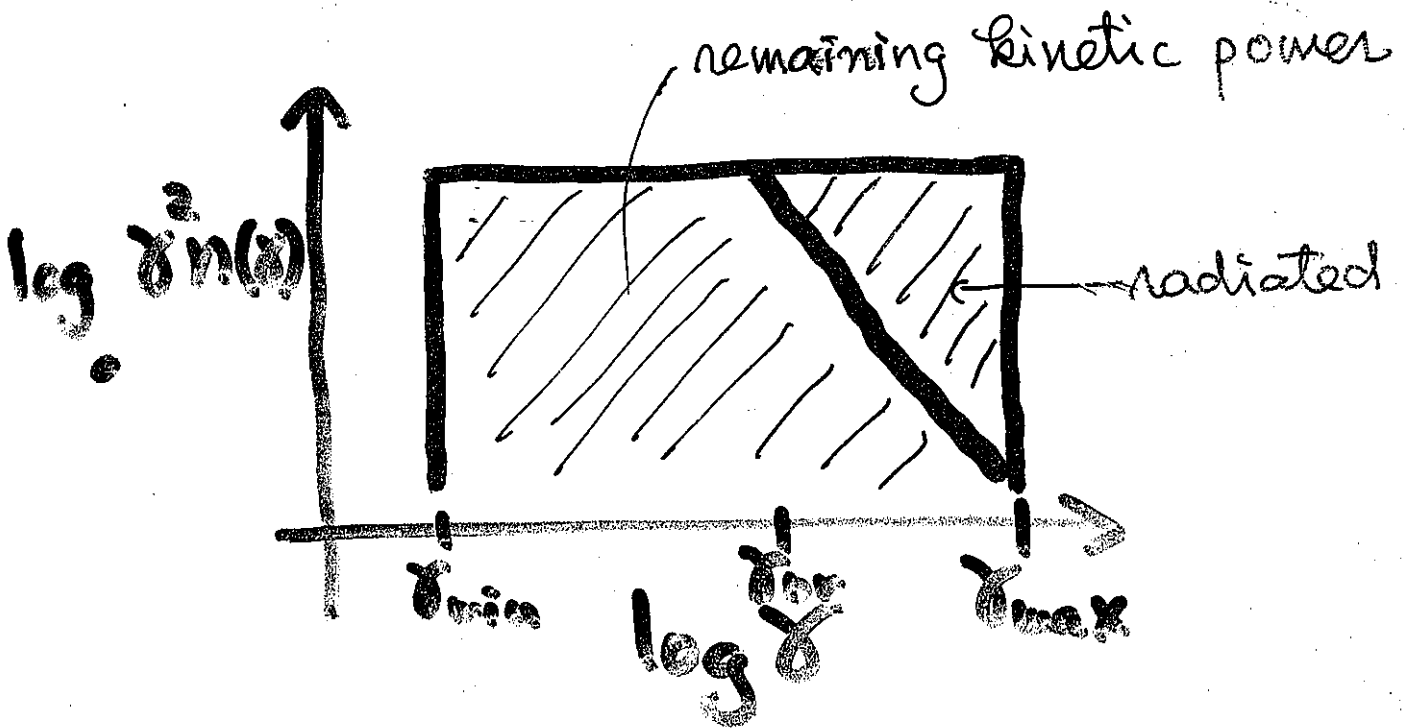
$$\gamma_{\max} m c^2 = \frac{2}{27} eBR \quad (\text{in the shock rest frame})$$



$$d_{sh} \approx c \Delta t \rho^2 \frac{\rho}{\delta\rho}$$



Shock acceleration
injection to cooling
region



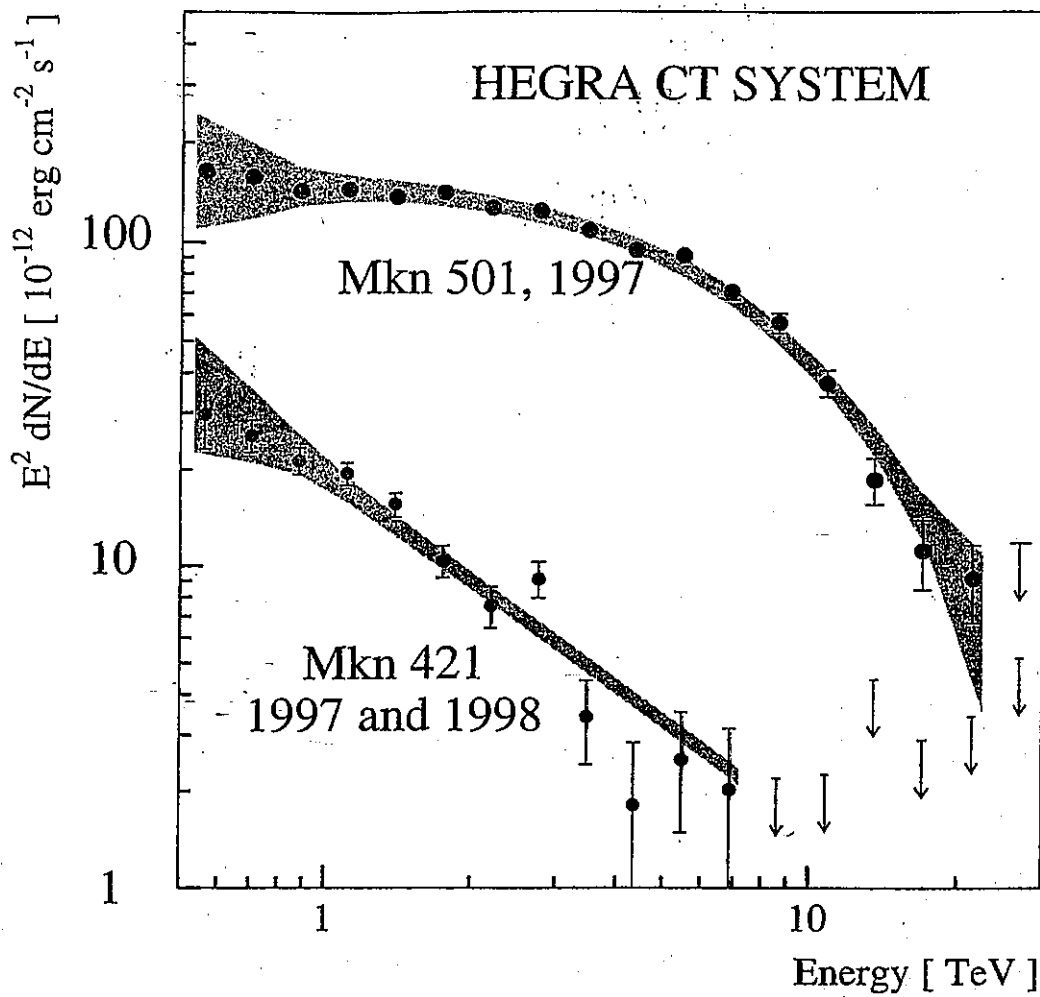


Fig. 9. The 1997 Mkn 501 and the 1997–1998 Mkn 421 spectral energy distributions. The hatched areas give the estimated systematic errors, except the 15% uncertainty in the absolute energy scale. Upper limits are at 2σ confidence level.

Blazar で陽子加速は起きているか？

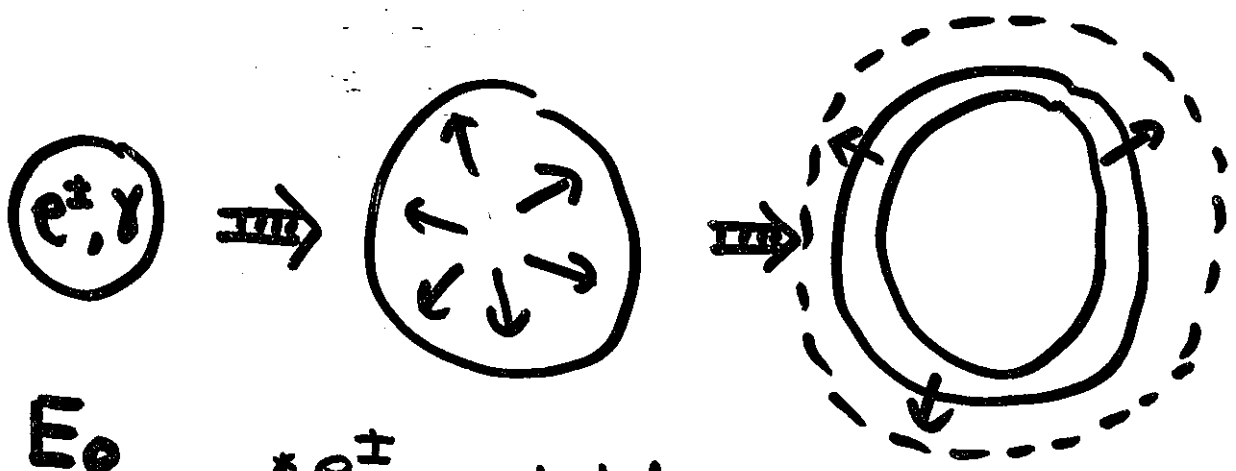
● 電子 (陽電子) モデルの根拠

- * X線と TeV との同時変動
- * TeV スペクトルは Mrk421 と Mrk 501 とで異なる。
- * jet の組成
 - $\left\{ \begin{array}{l} e^\pm \text{ 説} \\ e/p \text{ 説} \end{array} \right. \left\{ \begin{array}{l} \text{電波の偏光の性質} \\ \text{Lein の評価} \\ \text{bulk acceleration の容易さ} \end{array} \right.$

○ 陽子モデル

- * 電子モデルでは TeV- γ -ray spectrum の再現に問題
p- γ initiated shower, proton synchrotron を巻く。
- * 陽子モデルでは大きな磁場で fit する
 - $\left\{ \begin{array}{l} \text{磁場加速派の逃げ道} \\ \text{必要なパワーは何桁も増大} \end{array} \right.$
- * 陽子モデルはニュートリノ/放射を伴なう
 - $\left\{ \begin{array}{l} \gamma\text{-astronomy の target 探し} \\ \text{中性子の役割などの新奇さ} \end{array} \right.$

Cosmological Fireball



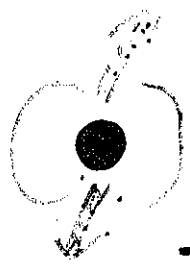
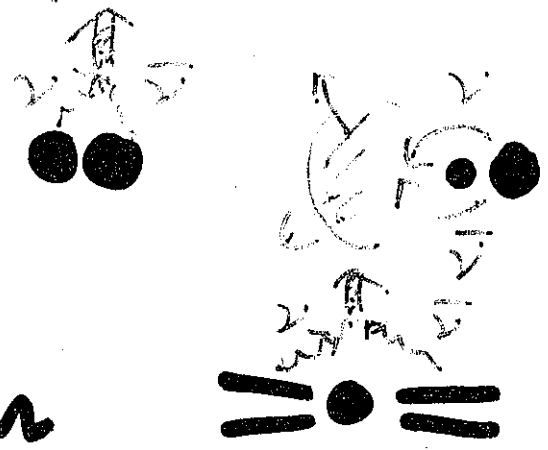
E_0
production

- * e^\pm annihilation
- * $\Sigma_T \lesssim 1$
- * Radiation \rightarrow Matter dominance

deceleration
by ambient
medium

production processes

- * NS merger
- * Failed SN
- * Newly Born Pulsar
- *



$$t_{\text{MDR}} \sim 200 \left(\frac{B}{3 \cdot 10^{15}} \right)^{-2} \left(\frac{P}{1 \text{ msec}} \right)^2 \text{ sec}$$

基本的なパラメータ

$$\eta \equiv \frac{E_0}{M_0 c^2} \sim 10^{-3} \frac{E_0 / 10^{51} \text{ erg}}{M_0 / M_\odot}$$

- $M_0 \gtrsim 10^{-3} M_\odot$: 非相対論的膨張
- $10^{-3} \gtrsim \frac{M_0}{M_\odot} \gtrsim 10^{-9}$; 相対論的膨張
- $10^{-9} M_\odot \gtrsim M_0$; prompt γ -rays

$\eta \gg 1$ を考慮す。

$$E_0 \sim a T_0^4 R_0^3$$

$$T_0 \approx 3 \cdot 10^{11} \text{ K} \frac{E_0 / 10^{51}}{(R_0 / 10^6)^3}$$

膨張 (radiation dominated)

$$T = T_0 \frac{R_0}{R}$$

$$E_{tr} = E_0 \frac{R_0^2}{R^2}$$

$$E_{kin} = E_0 = \Gamma E_{tr}$$

$$\Gamma = \frac{R}{R_0}$$

$$\bullet R_{T_{\text{ann}}} = R_{T_0} \frac{R_0}{R_{\text{ann}}} \sim m_e c^2$$

$$R_{\text{ann}} \sim 10^8 \text{ cm}$$

$$\bullet E_{\text{tr}} = E_0 \frac{R_0}{R_{\text{bd}}} \sim M_0 c^2 = \frac{E_0}{\eta}$$

$$R_{\text{bd}} \sim \eta R_0$$

この時期以降は $\Gamma \sim \eta \approx \text{const.}$
の膨張

• $\Sigma_T \sim n_e \sigma_T R \lesssim 1$ になる時期

$$n_e \sim \frac{M_0}{m_p R^3} \sim \frac{E_0}{R^3 \eta m_p c^2}$$

$$R_t \sim \left(\frac{E_0 \sigma_T}{\eta m_p c^2} \right)^{1/2} \sim 10^{15} \left(\frac{E_0}{10^{51}} \right)^{1/2} \eta^{-1/2} \text{ cm}$$

$\left\{ \begin{array}{l} R_t < R_{\text{bd}} \text{ for } \eta \gtrsim 10^6 E_{51}^{1/3} R_6^{-2/3} \\ R_t > R_{\text{bd}} \text{ for } \eta \lesssim \dots \end{array} \right.$

Deceleration by ambient matter

8.

$$E_0 \sim \eta^2 n_{\text{ext}} m_p c^2 R_{\text{dec}}^3$$

$$R_{\text{dec}} \sim 10^{18} E_{51}^{1/3} n_{\text{ext}}^{-1/3} \eta^{-2/3} \text{ cm}$$

$$\Delta t_{\text{obs}} \sim \frac{R_{\text{dec}}}{c} \cdot \frac{1}{\eta^2}$$
$$\sim 3 \cdot 10^7 E_{51}^{1/3} n_{\text{ext}}^{-1/3} \eta^{-8/3} \text{ sec}$$

$10^2 < \eta < 10^3$ の時

$$10^2 \text{ sec} > t_{\text{obs}} > 10^{-1} \text{ sec}$$

* 粒子加速 \rightarrow radiation は充分速くおこるか？

* micro-structure をどう説明するか？

* main burst と afterglow は何に対応するか？

通常のシナリオ

- Internal Shocks が GRB 本体
External Shock は Afterglow に対応
- Shock 加速で電子加速の効率が非常に大きく、
電子のシンクロトロン放射で観測を説明する。
- 陽子加速も必ず起きるので、宇宙線、ニュートリノ
も必ず生じる。

疑問

- * Internal shock の効率
- * 電子加速の効率
- * GRB スパイクの普遍性

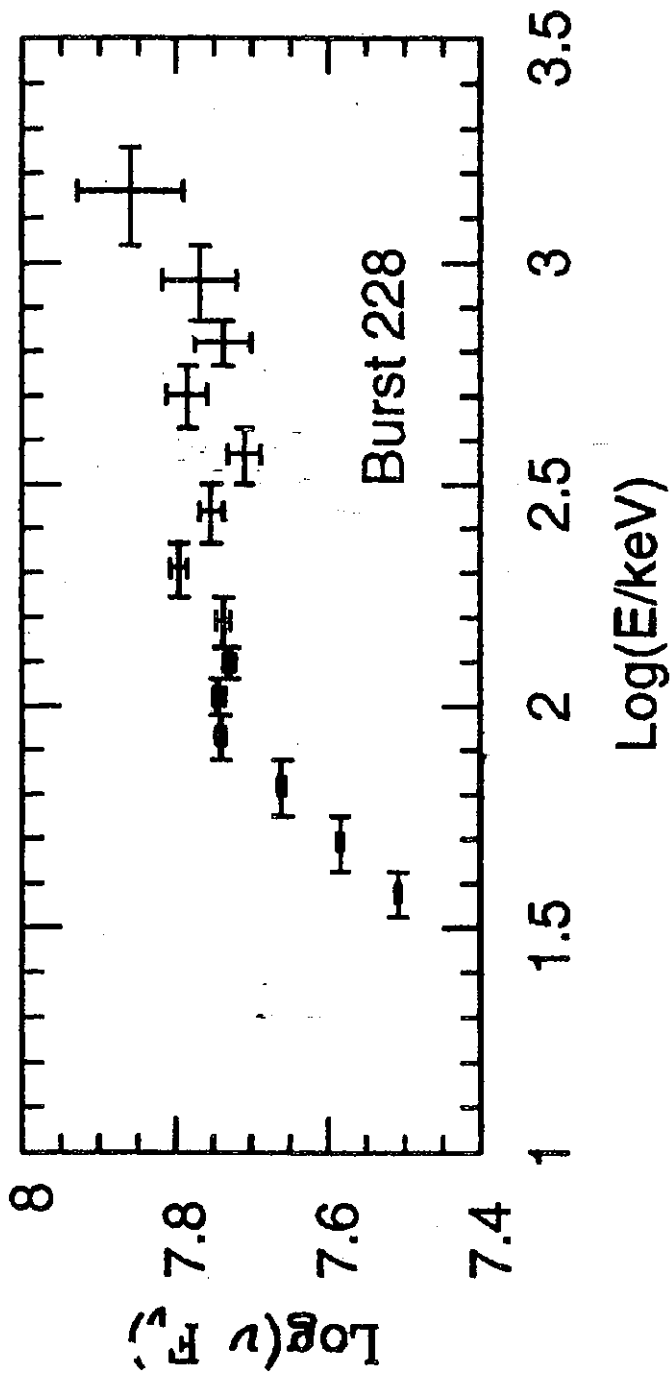


Figure 18.2: The spectrum of burst 228 from the BATSE 2 catalogue.

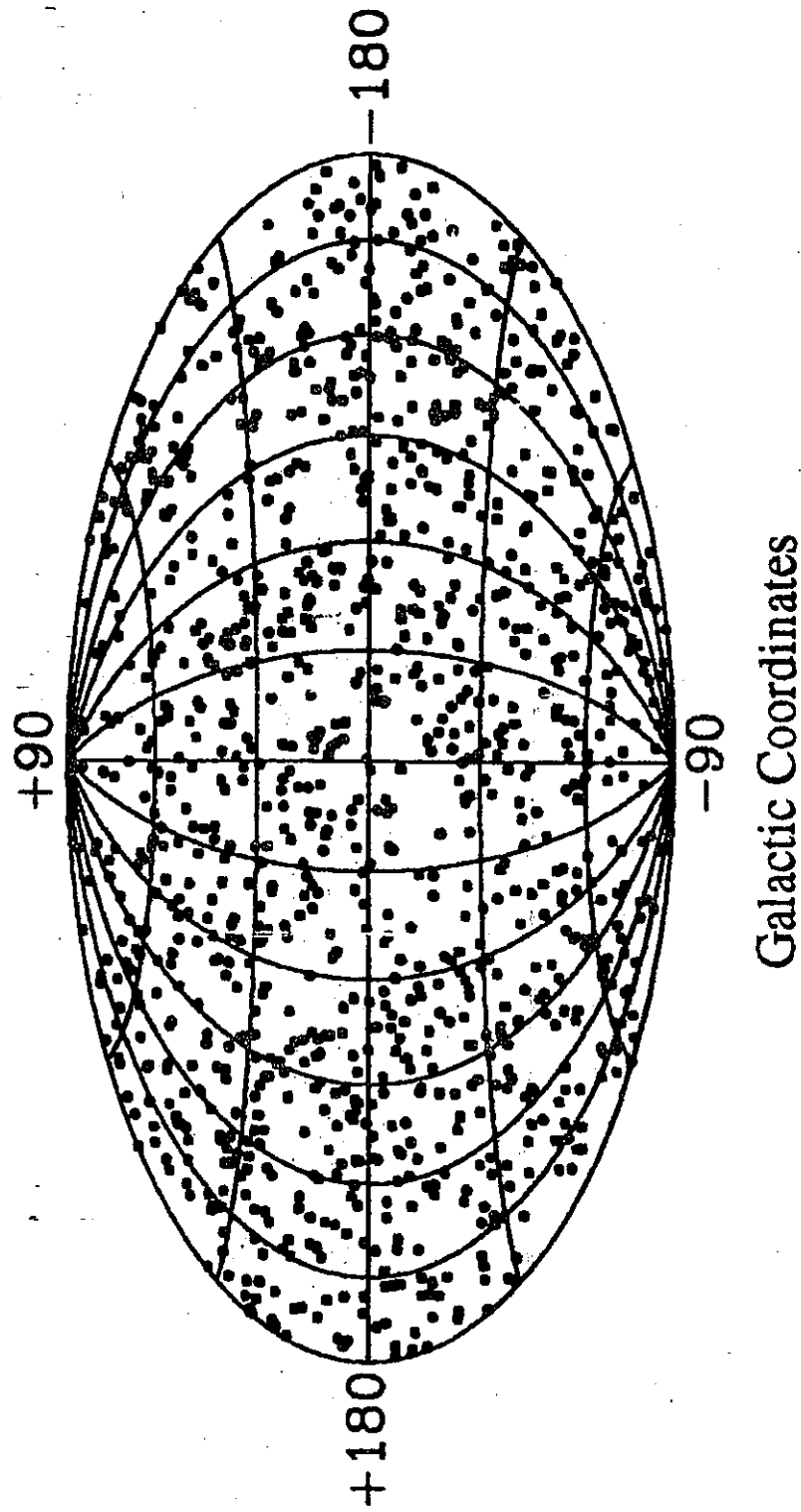


Figure 18.3: The Distribution of 1005 bursts on the sky.

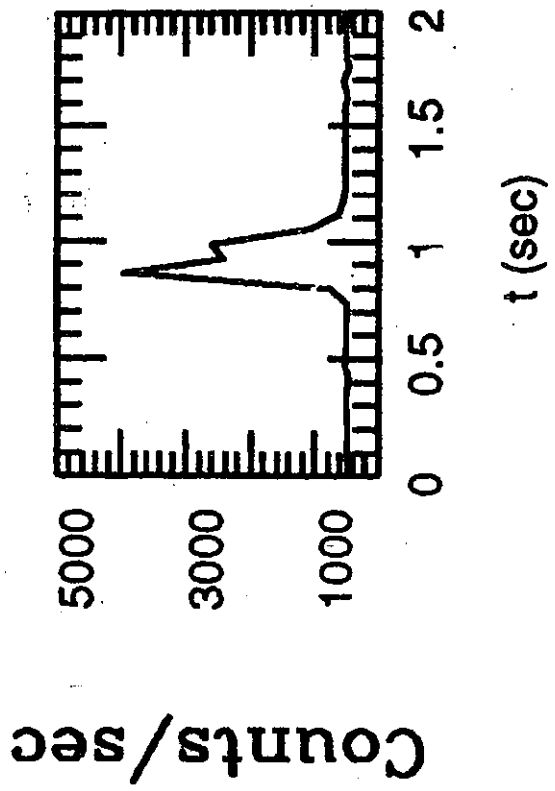
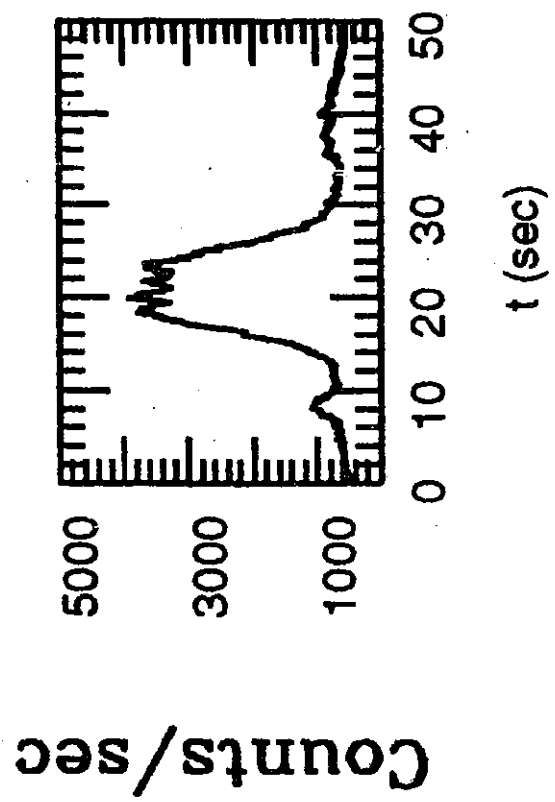
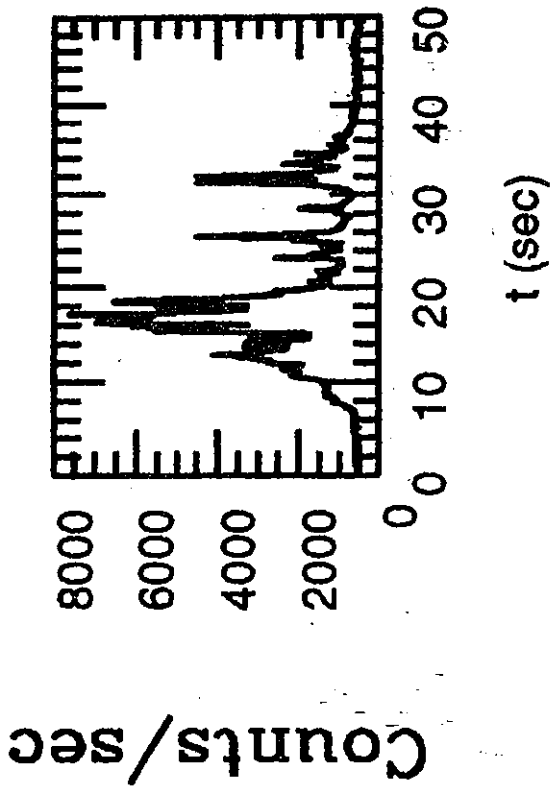
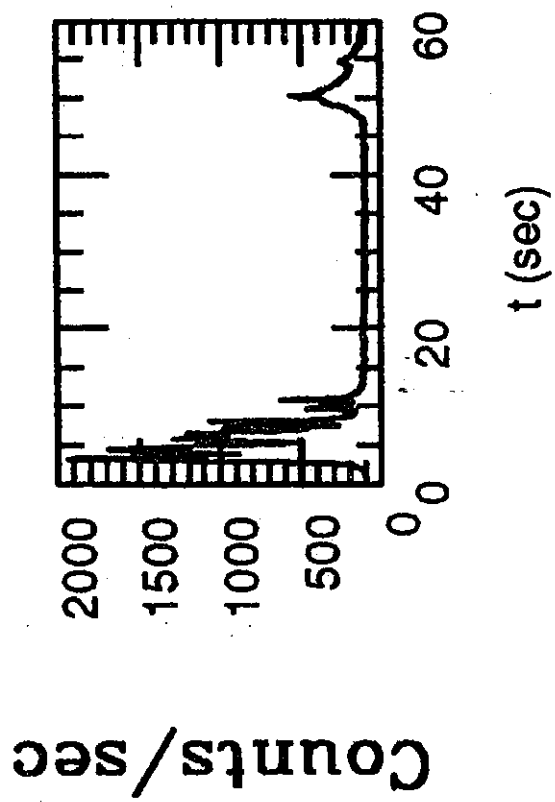


Figure 18.1: Temporal distribution of four bursts from the BATSE 2 Catalogue.